

# UC Irvine

## UC Irvine Previously Published Works

### Title

Cell damage by UVA radiation of a mercury microscopy lamp probed by autofluorescence modifications, cloning assay, and comet assay

### Permalink

<https://escholarship.org/uc/item/8n35r01d>

### Journal

Journal of Biomedical Optics, 1(2)

### ISSN

1083-3668

### Authors

Koenig, Karsten  
Krasieva, Tatiana B  
Bauer, Eckhard  
[et al.](#)

### Publication Date

1996

### DOI

10.1117/12.233373

### Copyright Information

This work is made available under the terms of a Creative Commons Attribution License, available at <https://creativecommons.org/licenses/by/4.0/>

Peer reviewed

# CELL DAMAGE BY UVA RADIATION OF A MERCURY MICROSCOPY LAMP PROBED BY AUTOFLUORESCENCE MODIFICATIONS, CLONING ASSAY, AND COMET ASSAY

Karsten K. König,<sup>†</sup> Tatjana Krasieva,<sup>‡</sup> E. Bauer,<sup>\*</sup> Ursula Fiedler,<sup>\*</sup> Michael W. Berns,<sup>‡</sup> Bruce J. Tromberg,<sup>‡</sup> and Karl O. Greulich<sup>\*</sup>

<sup>†</sup>Institute of Anatomy II, Friedrich Schiller University, 07743 Jena, Germany; <sup>‡</sup>Beckman Laser Institute, University of California, Irvine, CA 92715; <sup>\*</sup>Institute for Molecular Biotechnology, 07708 Jena, Germany

(Paper JBO-046 received Oct. 6, 1995; accepted for publication Feb. 14, 1996)

## ABSTRACT

Cell damage by low-power 365-nm radiation of a 50-W high-pressure mercury microscopy lamp was studied. Exposure of Chinese hamster ovary (CHO) cells to ultraviolet-A (UVA) radiation  $>10$  kJ/m<sup>2</sup> resulted in significant modifications of nicotinamide adenine dinucleotide (NADH) attributed autofluorescence and inhibition of cell division. Single-cell gel electrophoresis (comet assay) revealed UVA-induced single-strand DNA breaks. According to these results, UVA excitation radiation in fluorescence microscopy may damage cells. This has to be considered in vital cell microscopy, e.g., in calcium measurements.

**Keywords** UVA; NADH; autofluorescence; cloning assay; comet assay; electrophoresis; oxidative stress; UV microscopy; vital cell microscopy.

## 1 INTRODUCTION

Since the discovery of ultraviolet (UV) radiation in 1801 by the 24-year-old scientist, Johann Wilhelm Ritter from Jena, and the construction of the first “pure” UV lamp (“Wood’s lamp”), UV light has become a useful diagnostic and therapeutic tool in medicine and biology. For example, the well-established psoralen ultraviolet A (UVA) (PUVA) psoriasis therapy is based on application of the photosensitive drug Psoralen and UVA light. The Wood lamp is used to diagnose skin disorders, including the detection of skin bacteria, and UVA light is used as excitation radiation in cell fluorescence microscopy.<sup>1,2</sup>

On the other hand, UV radiation may induce genetic as well as nongenetic cell damage. UV-related damage to DNA and RNA is assumed to be either a result of direct absorption of UV photons, or of photo-oxidation processes after excitation of other cellular endogenous chromophores. Nucleic acids have major absorption bands in the spectral range between 200 and 300 nm (maximum around 260 nm). However, solar photons shorter than 290 nm (UVC) are absorbed by stratospheric ozone. UVB radiation (290 to 320 nm) induces DNA damage via formation of pyrimidine photoproducts and other nucleic acid base photoproducts. UVA (320 to 400 nm) is well known to induce the formation of reac-

tive oxygen species (i.e., singlet oxygen and oxygen radicals) by photodynamic action with certain endogenous chromophores as photosensitizers. This results in oxidative stress.<sup>3–6</sup> Major endogenous absorbers of UVA light are flavin coenzymes, the reduced pyridine coenzymes  $\beta$ -nicotinamide adenine dinucleotide (NADH) and  $\beta$ -nicotinamide adenine dinucleotide phosphate (NADPH), porphyrins, and heme-containing enzymes, including cytochromes. Membrane proteins absorb UVA photons poorly due to the absence of significant absorption maxima in the UVA spectral region. When exposed to UVA light, intracellular NAD(P)H emits in the blue-green spectral region. Free NAD(P)H fluoresces at  $\approx 460$  nm. When bound to proteins, the confirmation changes from a folded to an unfolded form, resulting in an increased fluorescence quantum yield and a blue-shifted fluorescence maximum at  $\approx 440$  nm. For example, binding of NADH to alcohol dehydrogenase results in a twofold fluorescence increase. Because fluorescent coenzymes act as highly sensitive bioindicators of respiratory chain activity, monitoring of NAD(P)H-attributed autofluorescence provides information on light-induced disturbances of metabolic function.<sup>2,7–10</sup>

The aim of this paper is the evaluation of cell damage by the UVA radiation that is used as an excitation source in fluorescence microscopy. Clas-

Address all correspondence to Karsten König, Phone: 49 3641 631820; fax: 49 3641 631249; e-mail: kkoe@mti-n-uni-jena.de

sic fluorescence excitation is the 365-nm radiation of a high-pressure mercury lamp. UVA effects on cellular metabolism were probed by monitoring the cellular redox state during exposure, by studying cell growth and reproductive behavior after exposure, and by detection of UVA-induced DNA damage.

DNA damage was detected by single-cell gel electrophoresis (SCGE), also called comet assay. Comet assay allows the sensitive detection of DNA strand breaks, differentiates between single- and double-strand breaks, and yields information on repair mechanisms.<sup>11–13</sup> The assay is based on migration of DNA molecules, which carry a net negative intrinsic charge, in a weak electric field. When embedded in a porous medium such as an agarose gel, the migration distance is nearly inversely proportional to the logarithm of the molecule length. Therefore, smaller DNA fragments (e.g., those induced by UVA exposure) migrate further toward the anode than larger ones. Intact DNA shows no significant migration. When stained with a fluorescent dye, DNA migration can be detected. The DNA pattern has the appearance of a comet with a head and a tail, indicating intact DNA and DNA fragments, respectively. The alkaline SCGE allows detection of “alkali labile sites” and single-strand breaks, whereas the neutral assay detects double-strand breaks. The comet assay has so far been used to detect chemical-, UVC-, UVB-, and ionizing radiation-induced DNA damage.<sup>14–17</sup> As few as one DNA break per  $10^{10}$  daltons can be detected.<sup>15</sup>

## 2 MATERIALS AND METHODS

### 2.1 CELLS

Chinese hamster (*Cricetulus griseus*) ovary cells (CHO-K1, ATCC no. 61) were used in the UVA experiments due to their rapid reproduction time of about 12 hr and their ability to grow in low cell concentrations. This allows clonal growth studies on single isolated cells. CHO cells were maintained in GIBCO's minimum essential medium (MEM) supplied with 10% fetal bovine serum. For autofluorescence and clonal growth studies, cells were grown in sterile Rose chambers consisting of two 0.17-mm coverslips as chamber windows, a silicon gasket with a 2-cm opening as spacer, and metal frames.

### 2.2 AUTOFLUORESCENCE MONITORING

Intracellular autofluorescence imaging was performed with an inverted epifluorescence microscope (Zeiss, Germany). Fluorescence excitation and UVA radiation was provided by the 365-nm line of a 50-W high-pressure mercury lamp. UVA power was measured in air behind the Neofluar 100× phase-contrast objective near the sample plane to be 1 mW (power meter: 818-UV, Newport Corp., Irvine, CA). The homogeneity and area of

the UVA radiation transmitted through the 100× objective was measured by polymer film embedded with UV sensitive spiropiran compounds. The photosensitive spiropiran compounds undergo reversible heterolytic bond breaks during UV exposure, resulting in fluorescent photoproducts with absorption bands in the blue, and lifetimes of several minutes.<sup>18</sup> A diameter of the circular UVA irradiation area of 0.190 mm was detected by confocal fluorescence imaging ( $\lambda_{\text{exc}} = 488 \text{ nm}$ ,  $\lambda_{\text{f}} > 510 \text{ nm}$ ). Therefore, the UVA intensity at the sample is about  $35 \text{ kW/m}^2$ .

Autofluorescence images were recorded in the spectral range of 430 to 470 nm using a thermoelectrically cooled, slow-scan CCD camera (Princeton Instruments) and processed with IP Lab software (Signal Analytics Corp.). Fluorescence acquisition time was chosen to be 1 s. Autofluorescence imaging was performed on cell monolayers in Rose chambers at 37 °C.

### 2.3 CELL SURVIVAL AND CLONAL GROWTH

Trypsinized CHO cells were injected in a very low concentration (about 100 cells/ml) into Rose chambers. After attachment to the bottom coverslip, six cells of each chamber were preselected and marked by scribing a 50- $\mu\text{m}$  circle around the cell on the outside of the chamber window using a diamond objective (Zeiss). Three of the preselected cells were exposed to focused UVA radiation (100×) 6 hr after injection into Rose chambers. The experimental conditions were the same as for autofluorescence studies. The other three unexposed cells served as controls. Cells in the chambers were maintained in an incubator (5%  $\text{CO}_2$ , 37 °C) for up to 5 days after exposure. Circled, selected cells were found again by means of low-magnification phase-contrast microscopy. The marked cells were observed in 24-hr periods for morphology and clonal growth. Clonal growth was considered to be unaffected by UVA exposure when the cell was able to form a clone of >25 cells after 72 hr.

### 2.4 ALKALINE SINGLE-CELL GEL ELECTROPHORESIS

For SCGE, attached CHO cells were exposed to 0.4% trypsin for 20 s, shaken, and placed in 6-mm cylindrical cuvettes ( $\approx 10^6$  cells/ml, 300 ml) filled with MEM medium. The cell suspension was stirred during UVA exposure (magnetic stirrer, H+P Labortechnik, München). The cuvette was kept in an ice-water bath during irradiation to minimize repair reactions. UVA exposure was performed with the unfocused 365-nm beam leaving the microscope (additional diaphragm instead of objective). UVA power was measured to be 22 mW. Considering a 1.5-cm<sup>2</sup> area of exposure at the sample, the mean intensity was  $150 \text{ W/m}^2$ . The time of exposure was chosen to be 0, 60, 180, 300, 600, and 1800 s.

The UVA-exposed cell suspension was centrifuged (rpm 1000), diluted with phosphate-buffered saline (PBS) (pH=7.4) to a final concentration of  $4.5 \times 10^5$  cells/ml, and mixed in a 1:5 ratio with 1% low-melting-point agarose at 45 °C (dissolved in PBS, A4018, Sigma, Germany). A microchamber consisting of a slide and 0.34-mm glass spacers was filled with the cell-agarose suspension and covered with a coverslip. After cooling, the coverslip was removed. The microchamber was immersed in lysis solution (2.5 M NaCl, 100 mM Na<sub>2</sub>EDTA, 10 mM Tris, 1% sodium sarcosinate, NaOH to adjust pH =10, 1% Triton X-100, 10% dimethylsulfoxide) and kept at 4 °C for 1 hr. Cells were then placed in a horizontal electrophoresis tank (0.33 M NaOH, 1 mM Na<sub>2</sub>EDTA, pH=14) for 15 min. Electrophoresis was performed at a field strength of 0.5 V/cm for 10 min (Bio Rad, Germany). The weak electric field leads to migration of broken DNA from the nucleus toward the anode, forming a "tail." Then microchambers were washed with Tris buffer, pH=7.5. Finally, cells embedded in agarose were stained with propidium iodide (PI, 2.5 mg/ml) for 30 min and examined using a fluorescence microscope (Axiovert M 135, Zeiss). The 536-nm radiation of a high pressure mercury lamp (broadband filter: 510 to 560 nm) was used for PI excitation; PI fluorescence (fluorescence maximum: 610 nm) was detected using an LP590 filter. Fluorescence was imaged with an intensified CCD video camera (model: Vario-Cam, PCO, Computer Optics GmbH, Kelheim) and analyzed with the software Komet, version 3.0 (Kinetic Imaging Ltd., Liverpool). This software analyzes more than 30 parameters of each comet, such as comet length, head size, and amount of DNA in head and tail by comparing fluorescence areas and intensities. We used the parameter tail moment, defined as the product of tail length and the amount of DNA in the tail, to characterize DNA damage. A total of 100 cells for each exposure time were evaluated. Experiments were performed in the dark.

### 3 RESULTS

#### 3.1 AUTOFLUORESCENCE MONITORING

Cells exhibited a weak fluorescence in the blue spectral region when excited with 365-nm radiation. Fluorescence arose mainly from mitochondria, as shown in comparative rhodamine staining tests. At first, UVA exposure led to a rapid fluorescence decrease—to 30 to 40% of the initial value. No morphological damage was observed with phase-contrast measurements as well as a trypan blue staining test. The cell autofluorescence reached a minimum after  $\approx 30$  s ( $\approx 1000$  kJ/m<sup>2</sup>), followed by a fourfold fluorescence increase within 10 min ( $\approx 20$  MJ/m<sup>2</sup>). Further irradiation results in a slow decrease. The increase in fluorescence intensity was accompanied by an autofluorescence relocalization. Interestingly, the whole cytoplasm started to show

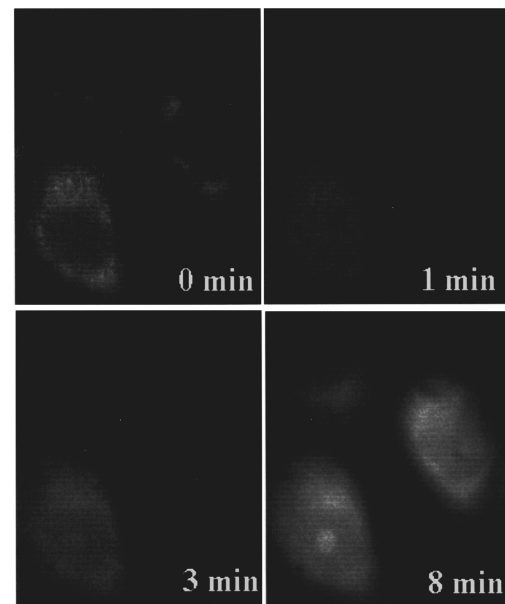


**Fig. 1** UVA-induced modifications of CHO autofluorescence.

up with intensities higher than those of mitochondrial fluorescence. The nucleus became fluorescent and, finally, the nucleoli turned out to be the most intense intracellular fluorescence sites (Figs. 1 and 2). Cells were no longer able to exclude trypan blue. They showed membrane blebbing and efflux of highly fluorescent material in the surrounding PBS medium.

#### 3.2 CLONING EFFICIENCY

Single interphase cells were exposed to UVA for different irradiation times and incubated for 5 days. A cell was considered to be unaffected by UV exposure if clones consisting of at least 25 cells were produced after 72 hr. The cloning efficiency of control cells (no UV exposure but the same experimental conditions and Rose chambers) was determined to be 94% (188 out of 200 cells produced clones). Significant inhibition of clonal growth was ob-

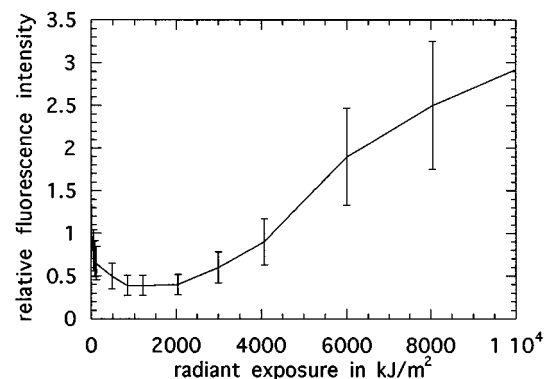


**Fig. 2** Mean cellular autofluorescence intensity versus UVA radiant exposure.

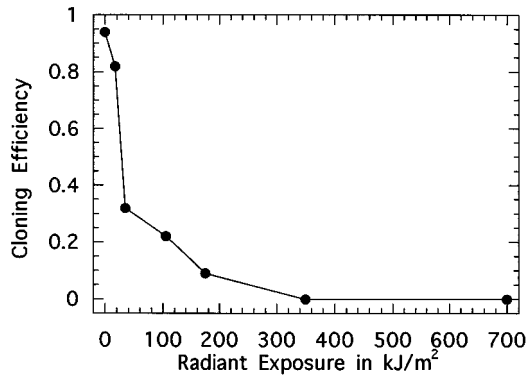


**Fig. 3** Mean cloning efficiency after UVA exposure ( $n=30$ ) versus radiant exposure.

served after UVA exposure. Figure 3 shows the mean dependence of cell cloning efficiency on UVA radiant exposure. UVA exposure times as low as 1 s ( $35 \text{ kJ/m}^2$ ) resulted in reduced cloning efficiency. Some of the exposed cells were able to undergo one cell division, but daughter cells were unable to divide. For exposure times  $>10$  s, all exposed cells failed to divide. Morphologically, these cells were visible as giant cells, dead cells with severe membrane damage (membrane blebbing), or shrunken dead cells.

### 3.3 COMET ASSAY

The DNA migration toward the anode was more pronounced in UVA-exposed cells than in control cells that experienced the same procedure but no UVA exposure. Figure 4 demonstrates a typical "comet" image of a cell exposed to UVA for 10 min in comparison with a "comet-free" unexposed cell. The comet tail reached a length of  $30 \mu\text{m}$  whereas the "head" had a dimension of  $26 \mu\text{m}$  (a larger size than the nucleus diameter prior to electrophoresis). In some cases the tail length can reach threefold values of the head. More accurate is the use of the parameter "tail moment," which considers the relative amount of extranuclear DNA (considering area and fluorescence intensity of the tail). The curve in Fig. 5 shows the mean tail moment versus radiant exposure. A significant increase occurred within 1 min of exposure ( $9 \text{ kJ/m}^2$ ). A 30-min UVA exposure ( $270 \text{ kJ/m}^2$ ) resulted in threefold higher tail moments than for the unexposed cells. Curve fitting according to the equation for exponential kinetics:

$$y = a + b[1 - \exp(-cx)],$$

where  $a$ =tail moment of unexposed cells,  $a+b$ =maximum tail moment, and  $c$ =rate constant, yields parameters  $a=3.4 \pm 0.4$ ,  $b=7.8 \pm 0.6$ , and  $c=(0.016 \pm 0.003) \text{ m}^2/\text{kJ}$  ( $R=0.993$ ). It should be mentioned that in the 100 cells investigated for each exposure time, a large variety in the value for the tail moment was observed. This fact is demonstrated in

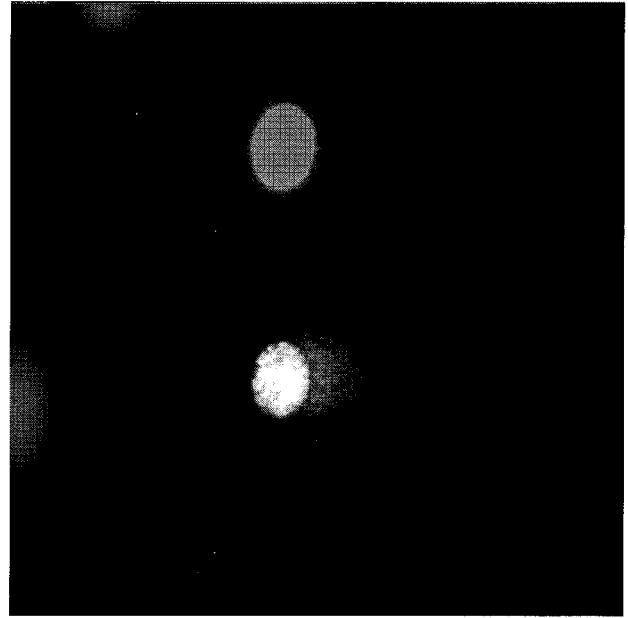


**Fig. 4** Fluorescence images of PI-labeled DNA of a single cell embedded in agar after lysis and electrophoresis. Up: non-UVA exposed cell; down: "comet image" of a UVA-exposed cell ( $270 \text{ kJ/m}^2$ ).

Fig. 6 showing tail moment histograms. A tail moment  $<4$  occurred even in 10% of the 30-min irradiated cells. However, 68% of the UVA-exposed cells in contrast to 4% of the unirradiated cells had tail moments  $>7$ .

## 4 DISCUSSION

We found that continuous-wave, low-power UVA radiation, which is used in fluorescence microscopy as excitation radiation, affects cell metabolism. This includes changes in cellular redox state, impaired cell division, and DNA damage. The autofluorescence intensity, indicative for the intracellular redox state, changed during UVA exposure. The initial decrease can be explained by a decrease in

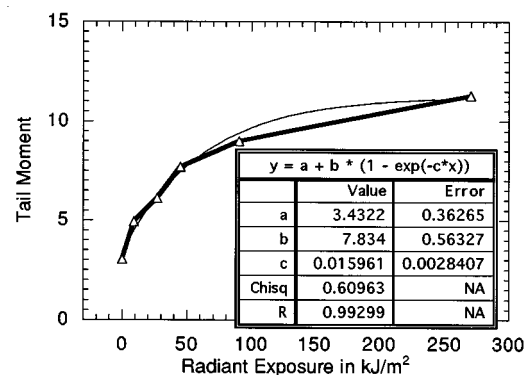


**Fig. 5** Mean tail moment versus UVA radiant exposure (alkaline comet assay).

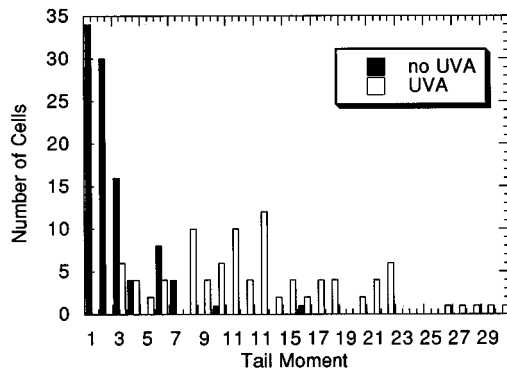


**Fig. 6** Tail moment histogram of UVA-exposed cells ( $270 \text{ kJ/m}^2$ ) and nonexposed cells.

NADH concentration due to photo-oxidation. UVA-induced transformation of NADH to oxidized NAD was found recently (unpublished results). The decrease of autofluorescence would therefore be indicative for a transformation of the cell in a more oxidized state. At this point, cells are still able to exclude trypan blue. Further UVA exposure (radiant exposures  $>1000 \text{ kJ/m}^2$ ) resulted in a strong fluorescence increase and fluorescence relocalization. This correlated with destructive effects, including severe damage to the outer membrane. An explanation for the onset of strong extramitochondrial fluorescence is the destruction of mitochondrial membrane and efflux of NAD(P)H in the cytoplasm. Mitochondrial damage could occur as a result of oxidative stress (UVA-induced formation of reactive oxygen species). The diffusion of photosensitizing mitochondrial chromophores, including NAD(P)H, in the cytoplasm and UVA exposure leads to damage to nuclear membranes and outer cell membranes. This induces NAD(P)H fluorescence in the nucleus and extracellular medium. Binding of NAD(P)H to the protein-rich nucleoli enhances the NAD(P)H fluorescence quantum yield and leads to intense fluorescence of nucleoli. Besides NAD(P)H binding to extramitochondrial proteins, the increase of cellular autofluorescence may be also a result of cell transformation in a reduced state as well as enhanced NAD(P)H biosynthesis.

A very sensitive indicator for cell damage is the cloning assay. Interestingly, we found that UVA radiant exposures as low as  $35 \text{ kJ/m}^2$  are sufficient to inhibit clonal growth. At these exposures, no significant autofluorescence modifications or morphological changes were detected. Therefore, the cloning assay seems to be more sensitive than on-line autofluorescence microscopy, transmission microscopy, and normally used viability tests such as the trypan blue exclusion test.

Low-power UVA radiation is able to induce breaks in DNA strands. We observed damage in some cells at radiant exposures as low as  $\approx 10 \text{ kJ/m}^2$ . Severe damage was detected for 90% of the

cells after  $270 \text{ kJ/m}^2$  of UVA exposure. Gedik, Ewon, and Collins<sup>15</sup> found, in the case of UVC exposure, single-strand breaks at radiant exposures as low as  $0.5 \text{ J/m}^2$ . UVA-induced inhibition of mitosis of fibroblasts at  $360 \text{ nm}$  was found for radiant exposures of about  $10 \text{ kJ/m}^2$  by Lubart et al.<sup>19</sup> This value agrees with our findings even though we used a different cell type.

Our results demonstrate clearly that the fluorescence excitation radiation used in cell fluorescence microscopy is capable of damaging the sample. This has to be considered in vital cell microscopy. A widespread use of vital cell fluorescence microscopy is the measurement of intracellular calcium in which fluorescent calcium indicators are excited with UVA light. New directions in vital cell microscopy are the excitation of UV transitions via two-photon excitation microscopy. This novel microscopy technique employs highly focused continuous wave or pulsed near-infrared (NIR) laser beams.<sup>20–22</sup> Out-of-focus cell regions experience only the relatively harmless low-intensity NIR radiation, whereas excitation of UV transitions by simultaneous absorption of two NIR photons occurs in the focal region (high intensity). This should result in reduced photobleaching and photodamage. However, up to now no systematic studies on cell damage induced by pulsed NIR microbeams exist.

#### Acknowledgments

This work was made possible, in part, through access to the Laser Microbeam and Medical Program (LAMMP) and the Clinical Cancer Center Optical Biology Shared Resource at the University of California, Irvine. These facilities are supported by the National Institutes of Health under grants RR-01192 and CA-62203, respectively. In addition, this work was supported by BMBF, Germany (Grant 0310708). The authors thank Dr. M. Boschmann (Rockefeller University), Dr. D. Celeda (IMB) and Dr. L. Wollweber (IMB) for stimulating discussions. Excellent technical support was given by Mrs. H. Fritzke and Mrs. H. Münster (IMB).

#### REFERENCES

1. K. König, "Johann Wilhelm Ritter - the discoverer of ultraviolet radiation," *Dermatol. Mon.schr.* **174**, 493–497 (1988).
2. K. König and H. Schneckenburger, "Laser-induced autofluorescence for medical diagnosis," *J. Fluorescence* **4**(1), 17–40 (1994).
3. T. G. Burchuladze, E. G. Sideris, and G. I. Fraikin, "Sensitized NADH formation of single-stranded breaks in plasmid DNA upon the action of near UV radiation," *Biofizika.* **35**, 722–725 (1990).
4. M. L. Cunningham, J. S. Johnson, S. M. Giovanazzi, and M. J. Peak, "Photosensitized production of superoxide anion by monochromatic (290–405 nm) ultraviolet irradiation of NADH and NADPH coenzymes," *Photochem. Photobiol.* **42**(2), 125–128 (1985).
5. M. Peak, J. Peak, and B. Carnes, "Induction of direct and indirect single strand breaks in human cell DNA by far- and near-ultraviolet radiations: Action spectrum and mechanisms," *Photochem. Photobiol.* **45**, 381–387 (1987).
6. R. M. Tyrrell, "The interaction of UVA radiation with cul-

- tured cells," *J. Photochem. Photobiol.* **4**, 349–361 (1990).
7. B. Chance and B. Thorell, "Localization and kinetics of reduced pyridine nucleotides in living cells by microfluorimetry," *J. Biol. Chem.* **234**, 3044–3050 (1959).
  8. C. Y. Guezennec, F. Lienhard, F. Louisy, G. Renault, M. H. Tusseau, and P. Portero, "In situ NADH laser fluorimetry during muscle contraction in humans," *Eur. J. Appl. Physiol.* **63**, 36–42 (1991).
  9. H. Schneckenburger, P. Gessler, and I. Pavenstädt-Grupp, "Measurement of mitochondrial deficiencies in living cells by microspectrofluorometry," *J. Histochem. Cytochem.* **40**(10), 1573–1578 (1992).
  10. H. Schneckenburger and K. König, "Fluorescence decay kinetics and imaging of NAD(P)H and flavins as metabolic indicators," *Opt. Eng.* **31**(7), 1447–1451 (1992).
  11. O. Östling and K. J. Johanson, "Microelectrophoretic study of radiation-induced DNA damages in individual mammalian cells," *Biochem. Biophys. Res. Comm.* **123**(1), 291–298 (1984).
  12. N. P. Singh, M. T. McCoy, E. E. Tice, E. L. Schneider, "A simple technique for quantitation of low levels of DNA damage in individual cells," *Exp. Cell Res.* **175**, 184–191 (1988).
  13. P. L. Olive, J. P. Banath, R. E. Durand, "Heterogeneity in radiation-induced DNA damage and repair in tumor and normal cells measured using the "Comet" assay," *Radiat. Res.* **122**, 86–94 (1990).
  14. R. R. Tice, P. W. Andrews, and N. P. Singh, "The single cell gel assay: A sensitive technique for evaluating intracellular differences in DNA damage and repair," in *DNA Damage and Repair in Human Tissues*, B. M. Sutherland and A. D. Woodhead, Eds., Plenum Press, New York (1990).
  15. C. M. Gedik, S. W. B. Ewen, and A. R. Collins, "Single-cell gel electrophoresis applied to the analysis of UV-C damage and its repair in human cells," *Int. J. Radiat. Biol.* **62**(3), 313–320 (1992).
  16. C. F. Arlett, J. E. Lowe, S. A. Harcourt, A. P. W. Waugh, J. Cole, L. Roza, B. L. Diffey, T. Mori, O. Nikaido, and M. H. L. Green, "Hypersensitivity of human lymphocytes to UV-B and solar irradiation," *Cancer Res* **53**, 609–614 (1993).
  17. A. de With, G. Leitz, and K. O. Greulich, "UV-B laser induced DNA damages in lymphocytes observed by single-cell gel electrophoresis," *J. Photochem. Photobiol. B* **24**, 47–53 (1994).
  18. A. S. Dvornikov, J. Malkin, and P. M. Retzepis, "Spectroscopy and kinetics of photochromic materials for 3D optical memory devices," *J. Phys. Chem.* **98**, 6746–6752 (1994).
  19. R. Lubart, Y. Wollman, H. Friedmann, S. Rochkind, and I. Laulicht, "Effects of visible and near-infrared lasers on cell cultures," *J. Photochem. Photobiol. B* **12**, 305–310 (1992).
  20. W. Denk, J. H. Strickler, and W. W. Webb, "Two-photon laser scanning fluorescence microscopy," *Science* **248**, 73–76 (1990).
  21. K. König, P. So, W. W. Mantulin, E. Gratton, M. W. Berns, and B. J. Tromberg, "Two-photon excited cellular autofluorescence induced by cw and femtosecond NIR microirradiation," *Proc. SPIE* **2628**, 12–19 (1995).
  22. K. König, H. Liang, M. W. Berns, and B. J. Tromberg, "Cell damage by near-IR microbeams," *Nature* **377**, 20–21 (1995).